International Journal of Remote Sensing
Vol. 30, No. 19, 10 October 2009, 5089–5108

Taylor & Francis
Taylor & Francis Group

Combining satellite imagery with forest inventory data to assess damage severity following a major blowdown event in northern Minnesota, USA

MARK D. NELSON*†, SEAN P. HEALEY‡, W. KEITH MOSER† and MARK H. HANSEN†

†US Department of Agriculture, Forest Service, Northern Research Station, St Paul, MN, USA

‡US Department of Agriculture, Forest Service, Rocky Mountain Research Station, Ogden, UT, USA

Effects of a catastrophic blowdown event in northern Minnesota, USA were assessed using field inventory data, aerial sketch maps and satellite image data processed through the North American Forest Dynamics programme. Estimates were produced for forest area and net volume per unit area of live trees pre- and post-disturbance, and for changes in volume per unit area and total volume resulting from disturbance. Satellite image-based estimates of blowdown area were similar to estimates derived from inventory plots and aerial sketch maps. Overall accuracy of the image-based damage classification was over 90%. Compared to field inventory estimates, image-based estimates of post-blowdown mean volume per unit area were similar, but estimates of total volume loss were substantially larger, although inaccessibility of the most severely damaged inventory plots may have depressed the inventory-based estimate. This represents the first application of state model differencing to storm damage assessment. The image-based procedure can be applied to historical archives of satellite imagery and does not require pre-disturbance field inventory data.

1. Introduction

Wind-related weather events cause damage to millions of hectares of forest land in the USA. The Forest Inventory and Analysis (FIA) programme of the US Department of Agriculture Forest Service is a national forest inventory (NFI) that is asked frequently to provide input into assessment of forest damage following these wind storms. While traditional plot-based inventory data can be used to characterize many aspects of a storm's impact upon a forest, FIA's fixed schedule of plot re-measurement can mean a delay of several years before this information is available. Sketch maps created through aerial survey can be produced more quickly, but their constituent attributes and precision generally are limited. Recently developed satellite-based change detection techniques may offer a compromise between sketch mapping and plot re-measurement in terms of response time and assessment depth. This study focused on a satellite image-based approach for mapping changes, which calibrates mapped disturbance with FIA inventory data, allowing a spatially and biophysically explicit representation of storm damage. Estimates derived from this approach were compared to estimates derived from both sketch mapping and plot re-measurement. A major windstorm that occurred in Minnesota, USA in 1999 was selected for investigation because adequate time had passed to allow subsequent collection of a

*Corresponding author. Email: mdnelson@fs.fed.us

International Journal of Remote Sensing
ISSN 0143-1161 print/ISSN 1366-5901 online
http://www.tandf.co.uk/journals
DOI: 10.1080/01431160903022951

rich ground inventory dataset. However, image-based techniques tested here could be applied in any situation where a storm has affected an area for which both pre- and post-storm imagery is available and forest inventory information is available from either pre- or post-storm periods.

1.1 *Immediacy and detail in storm assessments*

To make land management decisions, natural resource managers need information about extent, severity and recovery from damage following forest disturbance. Sources of such information include *ad hoc* field reconnaissance, aerial sketch mapping, remote sensing solutions and formal field inventories. Costs, timeliness and reliability of these information sources vary greatly. Post-disaster rapid assessment addresses this 'time to level-of-detail' trade-off that can be framed within an 'assessment–management–restoration–monitoring' continuum.

Initial assessments (available within days) are used to delineate damage areas, obtain gross estimates of potential damage and mobilize emergency resources. Management-driven mid-term data assessments (within weeks) obtain pre-disturbance data and images, identify variations in damage intensity, assist in initial mobilization of resources, and begin to categorize economic and other secondary impacts. Long-term analysis (within months) looks further toward management and begins to characterize restoration/mitigation opportunities. Monitoring efforts, like those pursued by NFIs, employ standardized sampling protocols and re-measurement of inventory plots (within years) for assessing general trends in forest disturbance.

Extent and severity of forest damage is affected by the susceptibility of trees and by the intensity and pattern of storm events. Both susceptibility and storm intensity can vary greatly over small distances, resulting in locally heterogeneous patterns of damage severity. Individual patches of blowdown in a Pennsylvania, USA study usually were less than 3 ha in area, with some patches less than 1 ha (Evans *et al.* 2007). Similarly, Foster and Boose (1992) determined that forest damage resulting from a 1938 hurricane in central Massachusetts, USA was spatially distributed primarily among patches less than 2 ha in area. Windthrow of individual trees is common and these occurrences are accelerated among residual trees bordering recent harvest clear-cuts. A study of partially harvested stands in British Columbia revealed that windthrow increased with increasing height–diameter ratio, crown density and fetch, while it decreased with increasing tree percentage live crown and post-harvest stand density (Scott and Mitchell 2005). Hurricane damage in central Massachusetts, USA, was related to vegetation height and composition and to site exposure (Foster and Boose 1992). In a Colorado study, Baker *et al.* (2002) observed that tree stem density, composition and structural stage had modest effects on the pattern of blowdown damage. Rich (2005) described forest dynamics and recovery following a major blowdown in northern Minnesota, USA. Studies such as these provide detailed information on individual blowdowns, but typically are not designed to meet NFI needs for timeliness and consistency.

NFIs provide consistent strategic information on extent and severity of damage resulting from forest disturbance. Valinger and Fridman (1999) used data from Sweden's NFI to assess risk of snow and wind damage to pine, spruce, and birch forests. NFI data also may be used for predicting susceptibility of forest trees to snow and wind damage, as was done by Jalkanen and Mattila (2000) with data from Finland's NFI. However, NFI estimates typically are valid for standard estimation units of moderate to large geographical extent and often require multiple years of field

data collection to produce precise estimates. Strategic inventories typically are not designed to produce spatially explicit, rapid assessments of forest disturbance events over smaller geographical extents, but such information is needed to provide for economically feasible salvage operations, mitigation of further ecological damage and delivery of information to the conservation community and general public.

In the state of Minnesota, USA, where this study was conducted, greater forest losses result from weather damage than from insects and diseases (Miles *et al.* 2007). Of Minnesota's 6.57 million ha of forest land, over 439 000 ha (approximately 6.7%) showed evidence of damage during field inventories between 1999 and 2003. About one third of this damage (121 603 ha) is attributed directly to wind effects (estimates obtained from Forest Inventory EVALIDator (http://fiatools.fs.fed.us/, 25 April 2008).

A catastrophic windstorm, named the 'Boundary Waters–Canadian Derecho', occurred across northern Minnesota, USA and western Ontario, Canada on 4 July 1999. Winds from this storm reached speeds of 130–160 km per hour, causing damage to tens of millions of trees and hundreds of thousands of hectares of forest land in the Superior National Forest (SNF) Boundary Waters Canoe Area Wilderness (BWCAW), USA and in adjacent Quetico Provincial Park, Canada (figure 1). This event triggered a need for information on areal extent of forest disturbance and severity of damage following the storm. Moser *et al.* (2007) analysed an intensified sample of FIA data to provide a snapshot of the entire BWCAW, including effects of the 1999 blowdown. However, the five-year cycle over which data were collected decreased the timeliness of this analysis and no comparable field data were available within the affected area from the period immediately preceding the blowdown event. Thus, a direct comparison of pre- versus post-blowdown forest composition and structure was not feasible using FIA data alone.

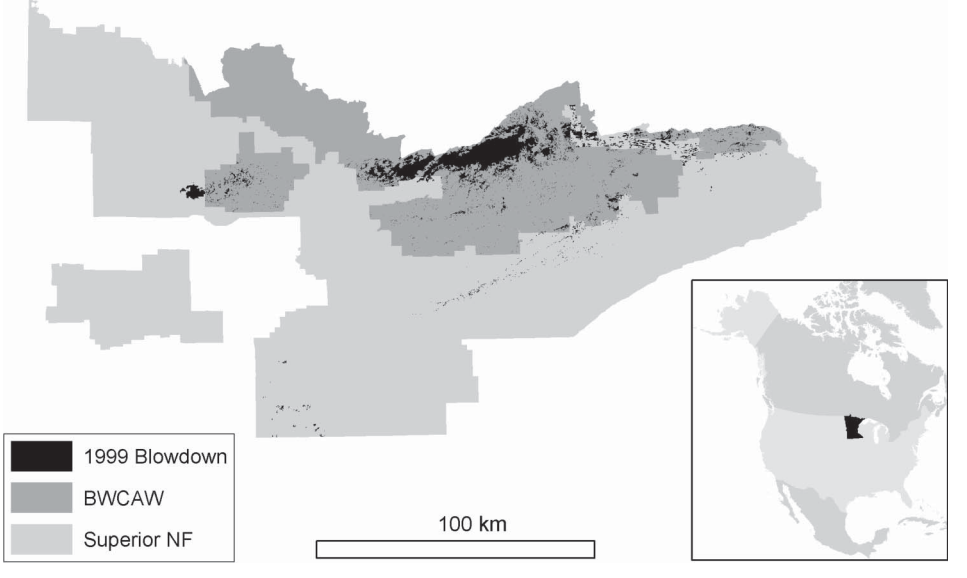

Figure 1. Superior National Forest, Boundary Waters Canoe Area Wilderness (BWCAW) and 4 July 1999 blowdown area; Minnesota, USA (inset).

1.2 *Combining inventory and satellite data to map storm damage*

Most satellite-based forest change detection algorithms have measured and mapped changes only in relative terms (e.g. high, medium, low damage) with an indefinite link to biophysical changes (Healey *et al.* 2007a). Spectral changes can be identified efficiently in a number of ways (e.g. Cohen *et al.* 2002, Sader *et al.* 2003, Kennedy *et al.* 2007), but calibration of those changes to specific changes in forest structure has been rare (although, see Olsson 1994, Häme *et al.* 2001). While modelling or imputation of forest variables using satellite imagery has gained broad usage (e.g. Hudak *et al.* 2002, Blackard *et al.* 2008, Tomppo *et al.* 2008), single-date mapping techniques do not necessarily translate easily into multi-temporal change detection problems. It has long been acknowledged that simple combination of independently produced maps from different time periods for change detection can result in an unsatisfactory compounding of error present in each map (Coppin and Bauer 1996, Howarth and Wickware 1981).

In an effort to minimize this compounded error problem, Healey *et al.* (2006) tested two methods of integrating multi-date satellite imagery with inventory information to biophysically calibrate change data while avoiding application of independent models for different periods. One method involved modelling basal area and cover changes directly as a function of Landsat spectral changes (simply: what change in biophysical variables is predicted by change in spectral variables). Because change was estimated with a single model, mapped changes were affected by only a single source of error. Measured prediction error for this technique was low. Unfortunately, this method, called 'direct change modelling', relied upon inventory information at different times to create and validate models of change. Because re-measured inventory data were available for neither the storm studied here nor many other storms that occur in the USA, we focused on the second method, 'state model differencing'. In this approach, radiometry of an image time series is carefully cross-normalized, and inventory information from throughout (or from just one point in) the time series is used to create a date-independent spectral model of a biophysical variable being used to describe change. Then, this single model is applied to each image in the time series, and differences in predictions from date to date are taken as estimates of change. Healey *et al.* (2006) reported relatively low prediction errors for state model differencing and, while any predictions of change will depend upon model quality, simplicity and flexibility of this method have appeal for storm assessments conducted in a 'rapid response' mode.

This paper represents the first application of state model differencing to storm damage assessment. FIA has recently entered into close collaboration with the North American Forest Dynamics project, an effort funded through the North American Carbon Program to map forest disturbance and re-growth across the continent (Goward *et al.* 2008). This collaboration has increased FIA's access to state-of-the-art radiometric and geometric image processing (Masek *et al.* 2008), and makes state model differencing in compressed time frames operationally feasible. This study tests compatibility of satellite-based storm damage measurements potentially available within a month of a storm and FIA's eventual re-measurement of inventory plots within the affected area. This information may be useful as FIA and other NFIs attempt to increase their responsiveness to requests for storm damage assessments.

2. Data and methods

2.1 *Study area*

The BWCAW comprises approximately 440 000 ha of the SNF, in northern Minnesota, USA (figure 1). A network of lakes and rivers within this forested landscape provided a water transportation route for early fur traders, most notably, French-Canadian voyageurs. Because of its unique history, ecological character and recreational value, the BWCAW is protected as a unit of the National Wilderness Preservation System. Approximately 72% (317 000 ha) of the BWCAW is forest land, 18% (77 000 ha) is open water and 10% is non-forest land, primarily wetlands that do not support tree cover. Forest types are nearly evenly distributed among deciduous forest and evergreen forest, with predominant tree species including paper birch (*Betula papyrifera*), quaking aspen (*Populus tremuloides*), black spruce (*Picea mariana*), jack pine (*Pinus banksiana*) and eastern white pine (*Pinus strobus*) (Moser *et al.* 2007).

2.2 *FIA plot-based estimates*

FIA defines forest land as lands currently or formerly supporting a minimum level of tree stocking (10%) and not developed for a non-forest use, such as agriculture, residential or industrial use. Forest land includes commercial timberland, some pastured land with trees, forest plantations, unproductive forested land and reserved, non-commercial forested land. FIA's definition of forest land also requires a minimum area of 0.405 ha (1 acre) and minimum continuous canopy width of 36.58 m (120 ft) (US Department of Agriculture Forest Service 2003). Although disturbance events can affect tree stocking and cover, they do not result in a reclassification of FIA forest land to non-forest unless the change is permanent.

FIA estimates of forest land area were obtained by multiplying total land area inventoried by mean proportion of forest land observed on FIA sample plots. These plots follow a nationally consistent design comprised of four fixed-radius circular subplots, selected from a nationally consistent hexagonal sampling frame with at least one plot selected for each 2400 ha hexagon (McRoberts *et al.* 2005). Estimates of net volume (hereinafter: 'volume') per unit area of live trees on forest land expressed in cubic metres per ha ($m^3\ ha^{-1}$) were calculated from measurements of tree diameter at breast height (DBH) and tree height for individual trees of 12.7 cm DBH or larger (Bechtold and Scott 2005, Reams *et al.* 2005). Estimates of area and mean volume per unit area, and their corresponding estimates of uncertainty were produced using a standard set of sample-based estimators employed by FIA (Scott *et al.* 2005).

Estimates of total volume loss were produced by

1. assuming that mean volume per unit area on post-blowdown undisturbed forest was representative of pre-blowdown mean volume per unit area on forest land that was subsequently damaged;
2. estimating pre-blowdown total volume on forest land subsequently damaged by multiplying estimates of damaged forest area by estimates of mean volume per unit area of undamaged forest;
3. estimating post-blowdown total volume for the area represented by plots with observed wind/weather damage; and
4. calculating difference between estimated pre- and post-blowdown total volume.

Standard errors of estimates of forest area, mean volume per unit area and total volume were used to determine 95% confidence intervals surrounding each plot-based estimate. Paired comparisons of estimates were interpreted as being statistically significantly different when their respective confidence intervals were non-overlapping. No standard errors or confidence intervals were produced for estimates of total volume loss because estimates of loss were calculated indirectly as the differences between estimates of total volume.

FIA's database was queried to obtain inventory field plot data collected between 1999 and 2003 (one full five-year cycle) within three counties of northern Minnesota, USA that encompass the blowdown area. Geographical Information System (GIS) data layers of inventory plot centre locations were created based on Global Positioning System (GPS) coordinates obtained during field data collection. GPS coordinates were collected and maintained in North American Datum of 1983. The sample of plots was further constrained to include only those plots located within the BWCAW and also within the geographical extent of Landsat World Reference System (WRS2) Path 27, Row 27 (P27R27). This study area encompasses the western extent of the 1999 blowdown, which includes much, but not all of the blowdown-affected area of the BWCAW.

Prior to 1999, FIA was not funded to measure sample plots in reserved areas such as the BWCAW. Therefore, FIA field plot data were unavailable for this area from years preceding the 1999 blowdown event and direct comparisons of pre- versus post-blowdown volume per unit area or total volume were not possible. Rather, plots were stratified by field-level observations of disturbance to compare mean volume per unit area and total volume estimates 'inside' versus 'outside' the blowdown area, assuming that pre-blowdown volumes were similar between these two strata. Additionally, plots were stratified using an ancillary geospatial dataset, following an approach of Woodall and Nagel (2007), who used a sketch map of blowdown severity to stratify BWCAW estimates of fuel loadings inside versus outside the 1999 blowdown. Stratification, as used in this study, is conducted for separating plots and pixels into two subpopulations—damaged versus undamaged forest—not for increasing the precision of estimates, as has been implemented in NFIs (McRoberts *et al.* 2006).

2.3 *FHP sketch map polygon-based estimates*

A sketch map of forest blowdown was obtained from the US Department of Agriculture Forest Service's Forest Health Protection (FHP) programme (Quinn Chavez, pers. comm.; FHP Aerial Survey Results Viewer: http://www.na.fs.fed.us/ims/aerial/viewer.htm (accessed 9 December 2008)). This sketch map was produced by FHP staff, who flew over the area in fixed-wing aircraft following the blowdown event, 'sketched' damage site locations on maps, and visually interpreted the severity of blowdown damage. This procedure involved labelling existing polygon delineations of Public Land Survey sections (each about 259 ha) with a damage severity class pertaining to forest cover within each and section, and disregarding non-forest land cover (e.g. lakes) present within sections. These maps were later digitized for use in a GIS.

FHP sketch map polygons were clipped to the BWCAW portion of P27R27 and constrained to damage type 'main stem broken/uprooted' and damage cause 'wind/tornado'. For these sketch map polygons, severity of damage was recorded as either low/medium (0–50% of trees in polygon broken or uprooted) or high (50–100% of trees

in polygon broken or uprooted) and pattern of damage was recorded as 'host type (i.e., forest) >50% and damage is patchy', meaning that more than half of each survey section was forested, and damage to forest was not ubiquitous. Aerial survey standards are from the Forest Health Monitoring programme (US Department of Agriculture Forest Service 1999).

Section polygons used for sketch mapping include areas of non-forest, notably lakes within the BWCAW study area. Furthermore, damage for all sketch map polygons was recorded as 'patchy', i.e. discontinuous; areal extent of damage within each sketch map polygon was less than 50% of forest land area for low/medium damage severity class and between 50% and 100% of forest land area for high damage severity class. Therefore, clipped and weighted estimates of blowdown damage area were produced using weights that were selected prior to producing or comparing estimates. This approach involved (1) clipping polygons to exclude open-water bodies as portrayed in a polygon geospatial dataset with 1: 24 000 scale, obtained from the Minnesota Department of Natural Resources, (2) assuming that remaining area within resulting polygons represented forest land, (3) assuming that midpoints for each FHP damage severity class (25% for low/medium class, 75% for high class) were representative of mean damage severity for each of the two classes, and (4) weighting the estimate of forest land area by these midpoints. Spatial operations were performed using a GIS. Estimates of mean volume per unit area, total volume and volume loss and their associated estimates of variance were not available from FHP sketch map polygons.

An assessment of classification accuracy was performed on the FHP sketch map damage polygons using FIA plots with wind disturbance as a reference dataset. Overall classification accuracy and kappa statistics were calculated (Jensen 1996: 248, 251).

2.4 *Satellite image-based estimates*

Landsat 5 Thematic Mapper (TM) and Landsat 7 Enhanced TM Plus (ETM+) images were obtained for P27R27. Annual or biennial TM and ETM+ images from 1985 to 2006 were converted to surface reflectance by the North American Forest Dynamics (NAFD) Programme (Goward *et al.* 2008) using National Aeronautics & Space Administration (NASA)'s Landsat Ecosystem Disturbance Adaptive Processing System (LEDAPS: Masek *et al.* 2008). Following this atmospheric correction, an automated ordination procedure (multivariate alteration detection: Canty *et al.* 2004, Schroeder *et al.* 2006) was used to identify pseudo-invariant pixels and enhance relative normalization in the radiometry among images in the time series. Resulting images have 28.5 m spatial resolution and Universal Transverse Mercator (UTM) projection.

NAFD protocols include methods for making spatially explicit (map-based) estimates of changes in above-ground forest biomass and carbon (Healey *et al.* 2007b). The NAFD approach involves (1) linking FIA plots to pixels within images having the same measurement year as the plots, (2) associating image pixel values with plot-based observations of a forest structural attribute, e.g. biomass per unit area or volume per unit area, and (3) producing models that estimate per-pixel attributes and that can be applied to each cross-normalized image in the time series dataset.

These protocols were adapted slightly for this study to constrain the time series to only one pre-disturbance image from 1998, acquired approximately 12 months prior

to the 1999 blowdown, and one post-disturbance image from 1999, acquired two weeks following the 1999 blowdown, thus simulating a rapid assessment scenario; for comprehensive retrospective studies, NAFD has developed methods (see Kennedy *et al.* 2007) for fully exploiting temporal context present in long time series. FIA plot data were available only since 1999 ($n = 939$) so spectral values were extracted from a single image acquired in 1999. Relying on the absolute correction-to-surface reflectance and further relative normalization, we then applied the model resulting from the 1999 extraction to the 1998 image. Models were produced separately for evergreen forest and for deciduous forest/mixed forest, partitioned by non-overlapping forest land cover class values from the 2001 National Land Cover Dataset (Homer *et al.* 2007). Results were combined into a single image for each year.

Also, estimates of change were made in terms of volume instead of biomass to allow for direct comparison with FIA estimates of volume. Pixel predictions of volume per unit area were modelled using a regression tree-based method combined with recursive linear regression as implemented in Cubist software package (www.rulequest.com). Boosting and pruning were used and decisions were made from a number of trees in combination with a regression-based technique. The same model (i.e. ensemble of 100 trees) was applied to both the 1998 and 1999 images.

Clouds and shadows, which covered a minimal fraction of the study area, were excluded from analyses. Given a prohibition of silvicultural practices within the BWCAW and local knowledge of disturbance history, we assumed that loss of volume within the study area between 1998 and 1999 was attributable to the 1999 BWCAW blowdown.

A threshold of volume per unit area loss was used to assign image pixels to two strata, thereby allowing comparison of estimates between damaged and undamaged forest land. Several authors have reported approaches for determining thresholds of damage classes. Healey *et al.* (2005) combined three tasseled cap transformations to produce a 'Disturbance Index' (DI) of forest disturbance, then used a supervised classification algorithm to accommodate image-specific thresholds of DI values to identify stand-replacing disturbances. Hudak *et al.* (2007) classified Landsat satellite image pixels as being affected by stand-replacing disturbance, as follows: (1) calculate a vegetation index for every pixel at two time periods; (2) produce an image of per-pixel difference in vegetation index between the two time periods; (3) estimate an image-wide standard deviation (SD) of per-pixel difference; and (4) apply a minimum threshold of two SD for identifying disturbance pixels. Rogan and Miller (2007) identified a gradient of change in canopy percentage cover from which change classes were labelled, including a 'no change' class. In this study, image pixels were assigned to either damaged (i.e. blowdown) or undamaged (i.e. non-blowdown) class using the following procedure. Using per-pixel volume per unit area estimates obtained from a modified NAFD protocol described above, (1) calculate estimated mean pre- and post-blowdown volume per unit area within a three pixel by three pixel moving window (focal mean) – a pixel window that reduces potential effects of image mis-registration and also corresponds to the approximate footprint of FIA field plot observations; (2) subtract per-pixel 1999 post-blowdown estimate from 1998 pre-blowdown estimate of focal mean volume per unit area; (3) estimate per-pixel percentage loss in focal mean volume per unit area; (4) visually interpret satellite imagery and aerial photography to identify local areas of forest blowdown and determine the corresponding minimum threshold of focal mean percentage volume per unit area loss, i.e. 30%; and (5) apply this 30% minimum threshold to the volume per

unit area loss image to produce a thematic classification of blowdown and non-blowdown pixels. This classification map was used to mask both the 1998 and 1999 volume maps, retaining only those pixels labelled as 'blowdown', i.e. that exceeded the 30% minimum threshold of focal mean percentage volume per unit area loss.

FIA plots with wind disturbance were used as a reference dataset for assessing overall classification accuracy and kappa statistics (Jensen 1996: 248, 251) for the image-based classification of blowdown and non-blowdown pixels. Image-based estimates of blowdown damage area were obtained by multiplying the number of blowdown pixels by the area of each pixel (0.081225 ha). Estimates of mean volume per unit area on blowdown pixels were obtained for both the 1998 and 1999 images. Estimates of loss of mean volume per unit area and total volume were obtained by subtracting the 1999 volume estimates from the 1998 volume estimates across all pixels labelled as blowdown. No estimates of uncertainty were produced for image-based estimates of blowdown area, mean volume per unit area, total volume or total volume loss. As was done for FIA plots, image pixels were stratified separately using a sketch map dataset of blowdown intensity.

2.5 *Comparisons*

FIA plot-based estimates of blowdown forest area were compared to estimates obtained from satellite images and FHP sketch maps. Estimates of pre- and post-blowdown mean volume per unit area were compared and are reported as significantly different if satellite image-based estimates fell outside 95% confidence intervals surrounding FIA plot-based estimates. Because confidence intervals could not be produced for the image-based estimates, these comparisons tend to indicate differences when none exist, and thus are conservative tests of difference.

Pixel-based estimates of forest volume were available pre- and post-blowdown, allowing for a direct assessment of loss of mean volume per unit area and total volume. FIA plot data were available only post-blowdown. Thus, estimates of loss of mean volume per unit area and total volume were not directly comparable between plot- and pixel-based estimates.

Plot-based estimates of mean volume per unit area and total volume on damaged versus undamaged forest land were used as surrogates for pre- versus post-blowdown estimates. We deduced that this was a reasonable approach given findings from Moser *et al.* (2007), who reported that (1) mean volume per unit area within a 5 km buffer of blowdown was not significantly different from mean volume per unit area outside this buffer in the remaining portion of the BWCAW and (2) mean volume per unit area within the BWCAW was not significantly different from mean volume per unit area in the remainder of the SNF outside the BWCAW. From this we assert that non-blowdown mean volume per unit area was similar to pre-blowdown mean volume per unit area within SNF and BWCAW. Our criteria for success were based on statistical comparisons of damaged versus undamaged, and plot- versus pixel-based estimates.

3. Results

3.1 *FIA plot-based estimates*

Of 85 FIA plots on accessible forest land field-sampled within the study area during the 1999–2003 time period, nine showed evidence of wind disturbance, two showed

evidence of disturbance other than wind damage and 74 had no visible evidence of disturbance. An additional 12 plots were inaccessible and not field-sampled due to hazardous conditions. Field notes and aerial photo-interpretation were used to determine that seven of these 12 plots were forested with blowdown damage. These seven plots were assumed to be representative of the wind disturbance area and were pooled with the field-sampled plots, resulting in 16 plots used to estimate area of blowdown damage. On plots not field-sampled, post-storm volume per unit area was not inferred as readily as was presence of storm damage; these plots were not included in estimates of post-blowdown mean volume per unit area. One of 85 field-sampled plots had no measurable trees; thus, 84 plots were available for estimating volume per unit area, nine of which had wind/weather damage, 73 were undamaged and two had damage from agents other than wind/weather. Clouds and shadows comprised a minor fraction of the study area and no FIA plots within BWCAW had locations corresponding to image clouds or shadows. Estimates derived from FIA plots and from images with clouds masked were assumed to provide for valid comparisons.

Area of forest blowdown was estimated as 25 040 ha, representing 18.5% of forest land within the study area, with a 95% confidence interval of 25 040 $\pm$ 11 714 ha. Mean volume per unit area on forest land was obtained from 82 plots and estimated as 69.9 m^3 ha^{-1} (n = 73) for undisturbed forest, 44.4 m^3 ha^{-1} (n = 9) for forest with field observations of wind damage, 64.5 m^3 ha^{-1} (n = 19) within FHP sketch map damage polygons (excluding open water), 37.4 m^3 ha^{-1} (n = 6) for plots with field-observed damage and also located within sketch map polygons (excluding open water), and no estimate of volume per unit area for two plots damaged by agents other than wind/weather (figure 2). Estimates of mean volume per unit area on forest land with field-observed wind disturbance were significantly less than estimates for undisturbed forest land and

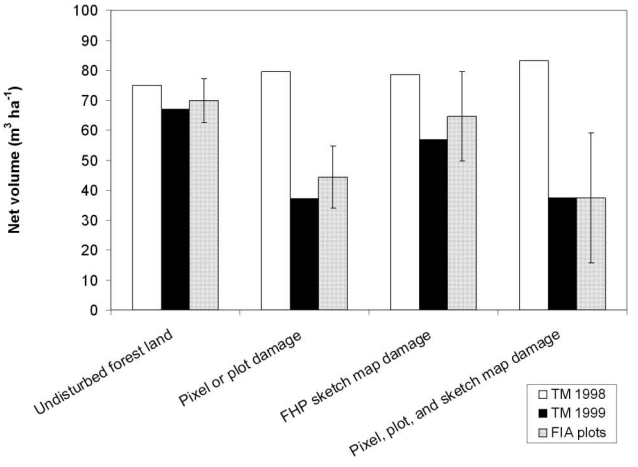

Figure 2. Landsat image-based (1998, 1999) and FIA plot-based (1999–2003) estimates of mean volume per unit area of live trees on forest land expressed in m^3 ha^{-1}, P27R27, BWCAW, Minnesota, USA: undamaged forest land, forest land where blowdown damage was observed on individual plots (wind/weather disturbance) or pixels (1998–9 loss of volume per unit area was $\geq$30% of mean volume per unit area), forest land within FHP sketch map damage polygons (excluding open water), and forest land having both plot- or pixel-damage and within FHP sketch map polygons (excluding open water). Error bars represent $\pm$95% confidence intervals surrounding plot-based estimates.

estimates for sketch map-only plots not having field evidence of wind disturbance (figure 2). Total volume loss from blowdown damage was estimated as 638 969 m^3.

3.2 *FHP sketch map polygon-based estimates*

The area of blowdown damage within FHP sketch map polygons was estimated as 27 561 ha after weighting by midpoints of damage severity classes, comprising slightly more than half of the non-water area within polygons labelled low/medium or high damage severity (48 400 ha). Of 16 FIA plots labelled as forest blowdown, 11 fell within and five fell outside FHP sketch map damage polygons. Of 79 FIA plots labelled as undamaged, 61 fell outside and 18 fell within sketch map damage polygons. Overall classification accuracy of FHP sketch map polygons relative to FIA plots was 75.8%, with a kappa statistic of 34.7. No estimates of volume were available from sketch map data.

3.3 *Satellite image-based estimates*

The regression tree-based models produced rms errors of 52.3 m^3 ha^{-1} (n = 362) for evergreen forest (82% of the mean value), 57.3 m^3 ha^{-1} (n = 577) for deciduous forest/mixed forest (70% of the mean value), and 55.4 m^3 ha^{-1} (n = 939) for all forest combined (74% of the mean value).

A comparison of figure 3(*a*) with 3(*b*) revealed substantial mean volume per unit area decrease from pre-blowdown (1998) to post-blowdown (1999) years within the north-east and west-central regions of the study area; these disturbance areas comprise a minority of the total study area (figure 3(*c*)). Focal mean volume per unit area

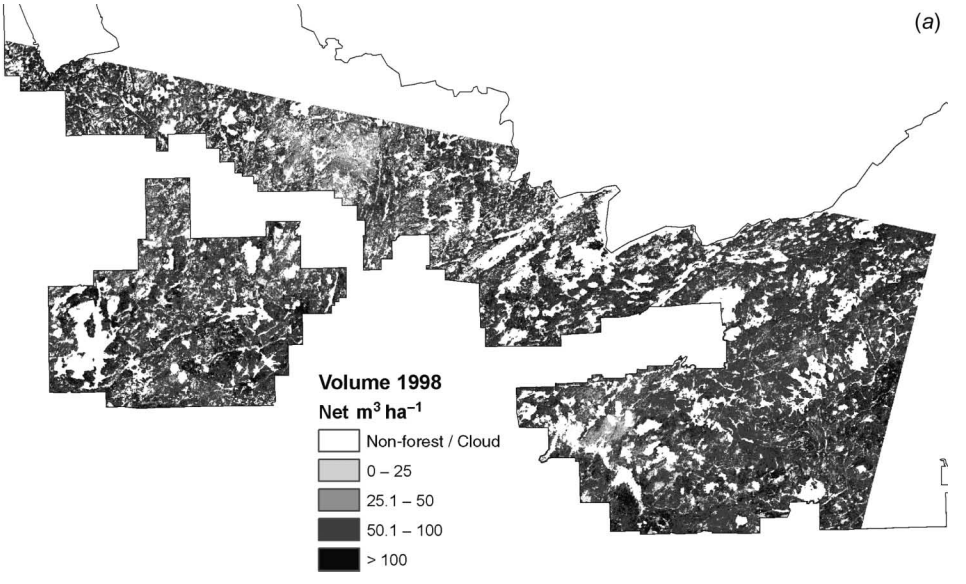

Figure 3. Volume per unit area of live trees on forest land expressed in m^3 ha^{-1}, BWCAW, Minnesota, USA, excluding lakes, clouds and non-forest land: (*a*) 1998 pre-blowdown volume; (*b*) 1999 post-blowdown volume; and (*c*) loss of volume between 1998 and 1999, resulting from blowdown damage.

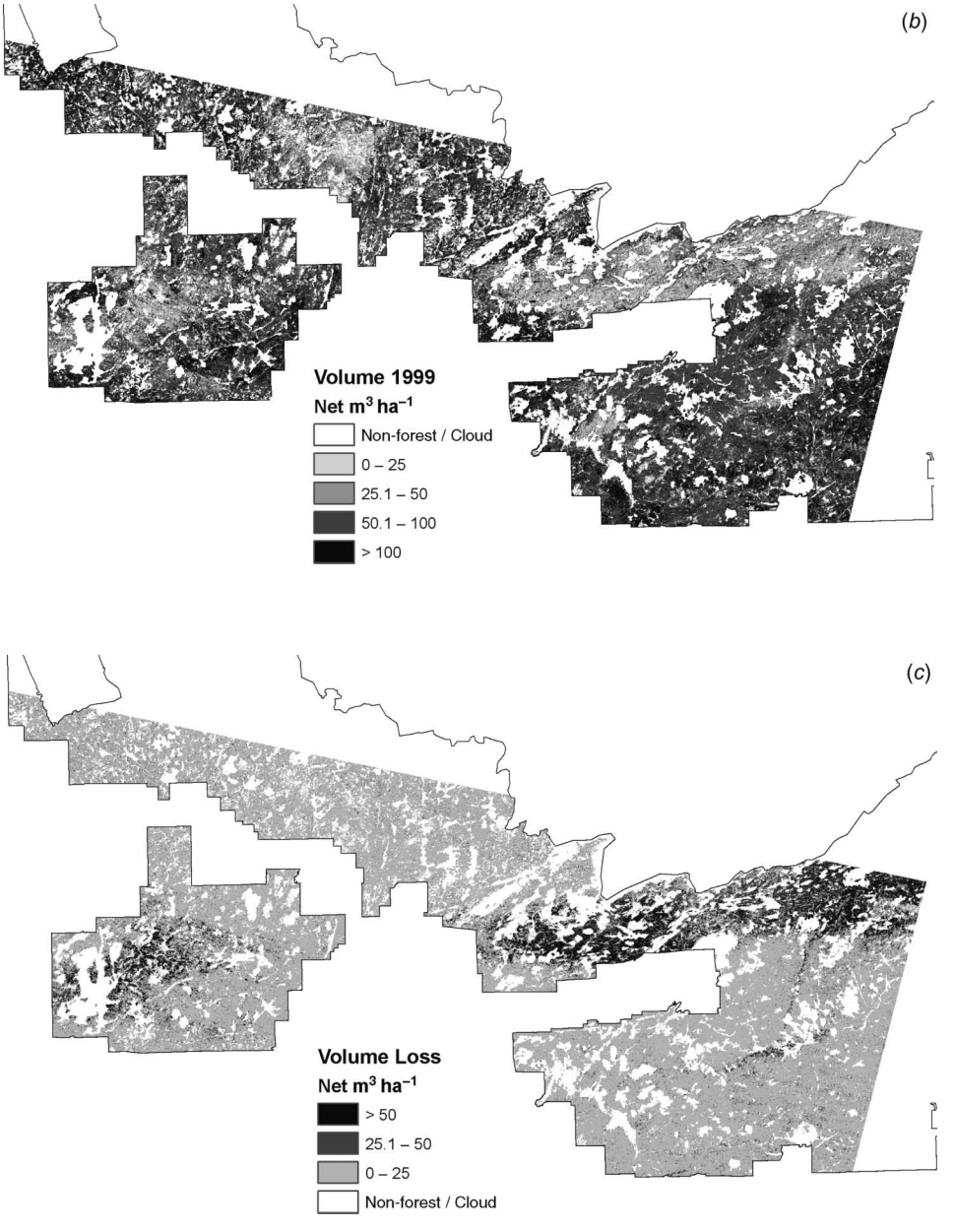

Figure 3. (*Continued.*)

loss of at least 30% was employed as a minimum threshold for labelling pixels as blowdown. Blowdown forest land area was estimated as 27 239 ha. Relative to FIA plots, overall accuracy of the image-based blowdown/non-blowdown classification was 91.6%, and the kappa statistic was 0.67.

Satellite image-based estimates of mean volume per unit area on undamaged forest land were 75.0 and 67.1 m^3 ha^{-1} for 1998 and 1999, respectively. When constrained to

only those pixels where loss exceeded 30%, post-blowdown mean volumes per unit area were 79.6 m^3 ha^{-1} for 1998 and 37.2 m^3 ha^{-1} for 1999. Mean volume per unit area within sketch map polygons was 78.5 and 56.8 m^3 ha^{-1} for 1998 and 1999, respectively. Pixels within sketch map polygons and also constrained by a minimum change threshold of 30% had mean volumes per unit area of 83.0 and 37.4 m^3 ha^{-1} for 1998 and 1999, respectively (figure 2). Total loss of volume attributed to blowdown was estimated as 1 154 512 m^3, equivalent to a loss of mean volume per unit area of 42.4 m^3 ha^{-1} on blowdown pixels.

3.4 *Comparison of estimates*

Estimates of forest blowdown area did not differ significantly between FHP sketch map-based (27 561 ha), Landsat satellite image-based (27 239 ha), and FIA plot-based (25 040 ha) estimates. Likewise, 1999 image-based estimates of mean volume per unit per ha fell within 95% confidence intervals of their corresponding plot-based estimates, suggesting no statistically significant difference between image- and plot-based estimates of post-blowdown mean volume per unit area (figure 2).

Estimates of mean volume per unit area on undisturbed forest land did not differ significantly between FIA plot-based (69.9 $\pm$ 10.3 m^3 ha^{-1}) and image-based estimates from 1998 (75.1 m^3 ha^{-1}) and 1999 (67.2 m^3 ha^{-1}) (figure 2). Image-based estimates of 1998 pre-blowdown mean volume per unit area appeared to be slightly greater for forest land subsequently damaged (79.6 m^3 ha^{-1}) than for forest not subsequently damaged (75.1 m^3 ha^{-1}), but the difference was not tested statistically (figure 2). The image-based estimate of 1998 pre-blowdown mean volume per unit area for forest subsequently damaged (79.6 m^3 ha^{-1}) was statistically significantly greater than the plot-based estimate for forest land with damage from wind disturbance (44.4 $\pm$ 15.0 m^3 ha^{-1}).

Within FHP sketch map polygons, the image-based estimate of 1998 mean volume per unit area (78.5 m^3 ha^{-1}) was not statistically significantly greater than the plot-based estimate (64.5 $\pm$ 21.7 m^3 ha^{-1}), except when estimates were also constrained to evidence of damage on individual pixels (83.0 m^3 ha^{-1}) and plots (37.4 $\pm$ 18.8 m^3 ha^{-1}).

Estimates of total volume loss resulting from blowdown were 638 969 and 1 154 512 m^3, from FIA plots and from satellite imagery, respectively.

4. Discussion

The historical archive of Landsat TM imagery enabled estimation of forest disturbance severity. Landsat TM imagery is available for years prior to establishment of FIA's annual forest inventory, allowing for historical estimates of forest disturbance not available from FIA data. The image-based procedure employed in this study requires availability of field inventory data corresponding to one or more years of TM imagery, but does not require that inventory data be available prior to disturbance or for every year of TM imagery. Even when pre-disturbance field data are available, estimates from the image-based procedure can be produced over smaller geographical extents than is possible from sample plots alone. Additionally, TM image maps portray more local detail in disturbance severity than is evident in plot-based inventory estimates. However, the image-based approach was not able to estimate uncertainty of population-level estimates of area, mean volume per unit area, total volume or volume change; the sample-based approach did produce corresponding estimates of uncertainty.

Image data available from the Landsat archive were carefully cross-normalized and combined with field data to create a date-independent spectral model of a biophysical variable. Maps and estimates of change in forest structure, following a major disturbance event, were produced by applying this model to multiple dates of imagery. We suggest that this approach may be employed elsewhere in the USA, given the extensive availability of the Landsat archive, and field data from the FIA programme. Similar results may be expected for other countries, if field data are available with similar measures of biophysical variables, and if these field observations can be associated with individual image pixels. Other optical satellite sensors may provide imagery as effective as Landsat imagery, but this was not tested. One advantage of the Landsat archive is its multi-decadal frame of availability, which provides for historical time-series analyses, such as those being conducted as part of NAFD.

A regression tree-based method was employed in this study, using a proprietary algorithm with no easy way to summarize variable importance. While the rapid response paradigm places a greater emphasis on operational efficiency than it does on fundamental research, we recognize the value of understanding relevant optical relationships and we recommend that future efforts employ more transparent methods. No statistical estimates of uncertainty were available for the image-based population estimates of damage area, mean volume per unit area, total volume, or volume loss. This is an area in which great benefit may be derived from further study.

It is recognized that methods taking advantage of the full temporal context available in a long image time series may have advantages over methods using only two dates (Kennedy *et al.* 2007). However, the simpler two-date model may be more practical in a compressed processing time frame following a catastrophic storm. The encouraging match observed here between satellite- and inventory-based estimates of storm area and damage suggests that simply acquiring a pre- and a post-storm image may be adequate.

Plot-based estimates of disturbance effects were assumed to be unbiased for sampled areas, given the sampling design employed by FIA. This appears to have been a valid assumption for estimates of forest blowdown area, given the similarity of estimates from FHP sketch map polygons, Landsat imagery and FIA plots. Plot-based estimates of damage area are derived from observations of presence or absence of wind disturbance, not on damage severity. Thus, inclusion of plots that were not field-sampled but were photo-interpreted as having damage likely provided a representative sample for estimating area of blowdown damage.

Overall classification accuracy of the image-based blowdown/non-blowdown classification was greater than 90%, and the corresponding kappa statistic was 0.7. FIA field observations of wind disturbance were used as reference data for assessing classification accuracy, and estimates of tree volume per unit area from these same plots were used to model per-pixel forest volume per unit area. Then a 30% minimum threshold of loss of mean volume per unit area was used to produce the blowdown/non-blowdown classification. Thus, we recognize the possibility that the reference data may not have been completely independent from the classification map.

Estimates of total volume loss differed substantially between pixel-based (1 154 512 m^3) and plot-based (638 969 m^3) approaches, a difference of about 80%. Although estimates of blowdown area were similar between the pixel-based (27 239 ha) and plot-based (25 040 ha) approaches, the pixel-based estimate of loss of mean volume per unit area (42.4 m^3 ha^{-1}) was substantially larger than the plot-based estimate (25.5 m^3 ha^{-1}).

Plot-based estimates of total volume loss were calculated as differences between two estimates of total volume. In contrast with estimates of storm damage area,

estimates of volume loss relied solely on field-sampled plots for estimating volume per unit area. Plots not sampled in the field often were inaccessible because of hazardous conditions for field survey crews (fallen and standing dead trees posing risks of bodily injury). The prospect that more heavily damaged plots were disproportionately not field-sampled raises a possibility that plot-based estimates of total volume loss within this study area may have been biased downward. If so, actual volume loss may be closer to the estimate obtained through the Landsat-based maps than the current plot-based estimate suggests. While it is difficult to know the degree to which the plot-based estimate of total volume loss may have been affected by inaccessible plots, this does highlight an ability of aerial and satellite-based monitoring to measure landscapes uniformly, assuming the availability of representative training data.

Aerial sketch map data provided a timely means for rapidly assessing forest disturbance and for enhancing subsequent plot- and image-based estimates. FHP sketch map polygons of disturbance severity were produced within one month following the blowdown event, although such data often are available within several days following catastrophic events. In our study, sketch map data proved useful for producing estimates of total blowdown area and for providing moderate improvement when stratifying image- and plot-based estimates of post-blowdown mean volume per unit area and total volume. These benefits were achieved after open water was excluded and after the remaining forest area was calibrated using weights associated with each class of blowdown damage. Errors of omission and commission obtained from a confusion matrix of plots and polygons provide support for the assumption of patchy, discontinuous forest damage within FHP sketch map polygons, and for justification to weight estimates of area by damage class midpoints. It is unknown whether this weighting approach would perform similarly for forest land having differing characteristics of composition, structure or disturbance patterns. The plot-based estimate of mean volume per unit area within sketch map damage polygons was not significantly less than for undamaged forest land and the image-based estimate within sketch map polygons appeared to be only moderately less than the pre-blowdown estimate. We surmise that the relative insensitivity of mean volume per unit area estimates to stratification with sketch map polygon was attributable to the heterogeneity of damage within large sketch map polygons. This scale of aerial survey data should be considered when using a GIS to constrain estimates of forest disturbance within ancillary polygon boundaries.

FIA plot-based estimates and corresponding image-based estimates of mean volume per unit area were not statistically significantly different from one another for: undamaged forest land, areas of site-specific damage, areas within blowdown polygons and combinations thereof. This suggests that acceptable estimates of loss of mean volume per unit area following forest blowdown can be obtained by differencing satellite image-based estimates of pre- and post-blowdown volume, at least for our study area, and likely for other areas having similar forest composition, structure and disturbance regimes.

Image-based estimates of post-blowdown forest damage area and total volume loss were dependent upon a threshold of minimum percentage loss of focal mean volume per unit area. The threshold of 30% employed in this study was obtained by visually interpreting other imagery to identify locations of blowdown damage and determining the mean volume per unit area loss threshold that portrayed these same areas. Previous estimates of forest damage area and volume for this study area were based on a threshold of focal mean volume per unit area loss that exceeded 1 SD of mean

volume per unit area change (Nelson *et al.* 2007). An estimate of 1999 post-blowdown mean volume per unit area for pixels exceeding the 1 SD threshold was 37.2 m^3 ha^{-1}, which is similar to the estimate of 36.1 m^3 ha^{-1} reported in this study for pixels exceeding the 30% threshold.

Statistical power of reported comparisons was low, which is evident by wide confidence intervals surrounding plot-based estimates. Furthermore, no confidence intervals were estimated for image-based estimates, so comparison tests could indicate differences when none existed. Thus, substantial deviations from a plot-based estimate could be reported as being not statistically significantly different. However, both sketch map- and image-based estimates of blowdown damage area were within 10% of the plot-based estimate. Image-based estimates of mean volume per unit area in undamaged forest and blowdown forest were within 7% and 16%, respectively, of plot-based estimates. These differences likely are of minor practical importance when conducting rapid assessments of forest disturbance.

Low statistical power was symptomatic of using plot data from a strategic inventory, collected at a moderate sampling intensity, but used to produce estimates over atypical estimation units. Although no estimates of uncertainty were produced for image-based estimates, similarity of image- and plot-based estimates of damage area and mean volume per unit area, and ability to rapidly produce small-area estimates from imagery provide an attractive approach to augmenting sample plot-based strategic inventories following forest disturbance events.

Storm assessment methods investigated here each have attributes making them logical sources of information under different circumstances. Aerial sketch maps often are created within days of a disturbance event. Although the FHP sketch maps include some areas of undamaged forest, they do provide spatially referenced information capable of supporting rapid response decisions. Mapping disturbance area and volume loss with field-calibrated Landsat or other imagery is the least expensive option explored and also provides spatially explicit information.

Further, while acquisition of satisfactory post-storm imagery may take weeks or months (the current example could have been completed in approximately four weeks), estimates of storm-affected forest area and volume in this case have been compatible with assessments from field surveys that took years to complete. Systematic surveys, while vulnerable to bias if storm effects create large numbers of inaccessible plots, are critical both in determining error bounds for final storm assessments and in providing calibration data for other methods. As options for catastrophic storm assessment are considered, respective strengths of these approaches should be judged in relation to data needs, time constraints and available resources.

5. Conclusions

Four conclusions can be drawn from this study.

1. Estimates of forest blowdown area were similar among three sources – FHP sketch maps, image pixels and FIA plots – but only after sketch maps were weighted by midpoints of damage severity and forested FIA plots not field-sampled were included.
2. Satellite image-based estimates of post-blowdown mean volume per unit area were similar to corresponding estimates produced from FIA field plot data, but image-based estimates of total volume loss were greater than estimates obtained

from FIA plots. Plot-based estimates possibly were affected adversely by a number of blowdown plots not field-sampled due to hazardous field conditions.

3. Image and plot-based estimates were improved only moderately by stratifying on aerial sketch map polygons.
4. The NAFD approach of modelling per-pixel tree volume per unit area by combining FIA field data with Landsat TM satellite imagery may provide for timely and spatially explicit estimates of forest disturbance effects.

Acknowledgements

The authors thank the US Department of Agriculture Forest Service, Superior National Forest for funding the intensification of the FIA plot sample within the BWCAW during the inventory years immediately following the blowdown; NASA Applied Sciences and Terrestrial Ecology Programmes for funding Landsat image acquisition, processing and applications development; and Quinn Chavez of US Department of Agriculture Forest Service Forest Health Protection programme for providing aerial sketch map geospatial data of Minnesota 1999 wind damage. The authors also thank the anonymous reviewers and the associate editor for prescribing substantial improvements to the manuscript.

References

Baker, W.L., Flaherty, P.H., Lindemann, J.D., Veblen, T.T., Eisenhart, K.S. and Kulakowski, D.W., 2002, Effect of vegetation on the impact of a severe blowdown in the southern Rocky Mountains, USA. *Forest Ecology and Management*, **168**, pp. 63–75.

Bechtold, W.A. and Scott, C.T., 2005, The Forest Inventory and Analysis plot design. In *The Enhanced Forest Inventory and Analysis Program – National Sampling Design and Estimation Procedures*, P.L. Patterson (Ed.), pp. 27–42 (Asheville, NC: US Department of Agriculture Forest Service, General Technical Report SRS-80).

Blackard, J.A., Finco, M.V., Helmer, E.H., Holden, G.R., Hoppus, M.L., Jacobs, D.M., Lister, A.J., Moisen, G.G., Nelson, M.D., Riemann, R., Ruefenacht, B., Salajanu, D., Weyermann, D.L., Winterberger, K.C., Brandeis, T.J., Czaplewski, R.L., McRoberts, R.E., Paterson, P.L. and Tymcio, R.P., 2008, Mapping U.S. forest biomass using nationwide forest inventory data and moderate resolution information. *Remote Sensing of Environment* (Remote Sensing Data Assimilation Special Issue), **112**, pp. 1658–1677.

Canty, M.J., Nielsen, A.A. and Schmidt, M., 2004, Automatic radiometric normalization of multitemporal satellite imagery. *Remote Sensing of Environment*, **91**, pp. 441–451.

Cohen, W.B., Spies, T.A., Alig, R.J., Oetter, D.R., Maiersperger, T.K. and Fiorella, M., 2002, Characterizing 23 years (1972–1995) of stand-replacing disturbance in western Oregon forest with Landsat imagery. *Ecosystems*, **5**, pp. 122–137.

Coppin, P.R. and Bauer, M.E., 1996, Change detection in forest ecosystems with remote sensing digital imagery. *Remote Sensing Reviews*, **13**, pp. 207–234.

Evans, A.M., Camp, A.E., Tyrrell, M.L. and Riely, C.C., 2007, Biotic and abiotic influences on wind disturbance in forests of NW Pennsylvania, USA. *Forest Ecology and Management*, **245**, pp. 44–53.

Foster, D.R. and Boose, E.R., 1992, Patterns of forest damage resulting from catastrophic wind in central New England, USA. *The Journal of Ecology*, **80**, pp. 79–98.

Goward, S.N., Masek, J.G., Cohen, W.B., Moisen, G.G., Collatz, G.J., Healey, S., Houghton, R.A., Huang, C., Kennedy, R., Law, B., Powell, S., Turner, D. and Wulder, M.A., 2008, Forest disturbance and North American carbon flux. *Eos, Transactions American Geophysical Union*, **89**, pp. 105–116.

Häme, T., Stenberg, P., Andersson, K., Rauste, Y., Kennedy, P., Folving, S. and Sarkeala, J., 2001, AVHRR-based forest proportion map of the Pan-European area. *Remote Sensing of Environment*, **77**, pp. 76–91.

Healey, S., Cohen, W.B., Zhiqiang, Y. and Kennedy, R.E., 2007a, Remotely sensed data in the mapping of forest harvest patterns. In *Understanding Forest Disturbance and Spatial Pattern: Remote Sensing and GIS Approaches*, M.A. Wulder and S.E. Franklin (Eds), pp. 63–84 (Boca Raton, FL: CRC Taylor & Francis).

Healey, S.P., Cohen, W.B., Zhiqiang, Y. and Krankina, O.N., 2005, Comparison of Tasseled Cap-based Landsat data structures for use in forest disturbance detection. *Remote Sensing of Environment*, **97**, pp. 301–310.

Healey, S.P., Moisen, G., Masek, J., Cohen, W., Goward, S., Powell, S., Nelson, M., Jacobs, D., Lister, A., Kennedy, R. and Shaw, J., 2007b, Measurement of forest disturbance and re-growth with Landsat and FIA data: anticipated benefits from Forest Inventory and Analysis' collaboration with the National Aeronautics and Space Administration and University partners. In *Proceedings of the Seventh Annual Forest Inventory and Analysis Symposium*, 3–6 October 2005, Portland, ME, R.E. McRoberts, G.A. Reams, P.C. Van Deusen and W.H. McWilliams (Eds), pp. 171–178. (Washington, DC: U.S. Department of Agriculture Forest Service, Gen. Tech. Report WO-77).

Healey, S.P., Yang, Z., Cohen, W.B. and Pierce, D.J., 2006, Application of two regression-based methods to estimate the effects of partial harvest on forest structure using Landsat data. *Remote Sensing of Environment*, **101**, pp. 115–126.

Homer, C., Dewitz, J., Fry, J., Coan, M., Hossain, N., Larson, C., Herold, N., McKerrow, A., VanDriel, J.N. and Wickham, J., 2007, Completion of the 2001 National Land Cover Database for the Conterminous United States. *Photogrammetric Engineering & Remote Sensing*, **73**, pp. 337–341.

Howarth, P.J. and Wickware, G.M., 1981, Procedures for change detection using Landsat. *International Journal of Remote Sensing*, **2**, pp. 277–291.

Hudak, A.T., Lefsky, M.A., Cohen, W.B. and Berterretche, M., 2002, Integration of lidar and Landsat ETM+ data for estimating and mapping forest canopy height. *Remote Sensing of Environment*, **82**, pp. 397–416.

Hudak, A.T., Morgan, P., Bobbitt, M. and Lentile, L., 2007, Characterizing stand replacing harvest and fire disturbance patches in a forested landscape: a case study from Cooney Ridge, Montana. In *Understanding Forest Disturbance and Spatial Pattern: Remote Sensing and GIS Approaches*, M.A. Wulder and S.E. Franklin (Eds), pp. 209–231 (Boca Raton, FL: CRC Taylor & Francis).

Jalkanen, A. and Mattila, U., 2000, Logistic regression models for wind and snow damage in northern Finland based on the National Forest Inventory data. *Forest Ecology and Management*, **135**, pp. 315–330.

Jensen, J.R., 1996, *Introductory Digital Image Processing: A Remote Sensing Perspective*, 2nd edn (Upper Saddle River, NJ: Prentice Hall).

Kennedy, R.E., Cohen, W.B. and Schroeder, T.A., 2007, Trajectory-based change detection for automated characterization of forest disturbance dynamics. *Remote Sensing of Environment*, **110**, pp. 370–386.

Masek, J.G., Huang, C., Wolfe, R., Cohen, W., Hall, F., Kutler, J. and Nelson, P., 2008, North American forest disturbance mapped from a decadal Landsat record. *Remote Sensing of Environment*, **112**, pp. 2914–2926.

McRoberts, R.E., Bechtold, W.A., Patterson, P.L., Scott, C.T. and Reams, G.A., 2005, The enhanced Forest Inventory and Analysis program of the USDA Forest Service: Historical perspective and announcement of statistical documentation. *Journal of Forestry*, **103**, pp. 304–308.

McRoberts, R.E., Holden, G.R., Nelson, M.D., Liknes, G.C. and Gormanson, D.D., 2006, Using satellite imagery as ancillary data for increasing the precision of estimates for the

Forest Inventory and Analysis program of the USDA Forest Service. *Canadian Journal of Forest Research*, **36**, pp. 2968–2980.

Miles, P.D., Jacobson, K., Brand, G.J., Jepsen, E., Meneguzzo, D., Mielke, M.E., Olson, C., Perry, C.H., Piva, R.J., Wilson, B.T. and Woodall, C., 2007, *Minnesota's Forests 1999–2003 (Part A)*, pp. 92 (Newtown Square, PA: US Department of Agriculture, Forest Service, Northern Research Station).

Moser, W.K., Hansen, M.H., Nelson, M.D., Crocker, S.J., Perry, C.H., Schulz, B., Woodall, C.W., Nagel, L. and Mielke, M.E., 2007, *After the Blowdown: A Resource Assessment of the Boundary Waters Canoe Area Wilderness, 1999–2003*, pp. 54 (Newtown Square, PA: US Department of Agriculture, Forest Service, Northern Research Station).

Nelson, M., Healey, S., Moser, W.K. and Hansen, M., 2007, Integrating data from field inventories and satellite remote sensors to assess effects of forest blowdown. In *ForestSat 2007. Proceedings from a conference on forests and remote sensing: methods and operational tools*, 5–7 November 2007, Montpellier, France (Cemagref - UMR TETIS), p. 6; CD-ROM.

Olsson, H., 1994, Changes in satellite-measured reflectances caused by thinning cuttings in boreal forest. *Remote Sensing of Environment*, **50**, pp. 221–230.

Reams, G.A., Smith, W.D., Hansen, M.H., Bechtold, W.A., Roesch, F.A. and Moisen, G.G., 2005, The Forest Inventory and Analysis sampling frame. In *The Enhanced Forest Inventory and Analysis Program – National Sampling Design and Estimation Procedures*, P.L. Patterson (Ed.), pp. 11–26 (Asheville, NC: US Department of Agriculture Forest Service, General Technical Report SRS-80).

Rich, R.L., 2005, Large wind disturbance in the Boundary Waters Canoe Area Wilderness: forest dynamics and development changes associated with the July 4th 1999 blowdown. PhD thesis, University of Minnesota, St. Paul, MN.

Rogan, J. and Miller, J., 2007, Integrating GIS and remotely sensed data for mapping forest disturbance change. In *Understanding Forest Disturbance and Spatial Pattern: Remote Sensing and GIS Approaches*, M.A. Wulder and S.E. Franklin (Eds), pp. 133–171 (Boca Raton, FL: CRC Taylor & Francis).

Sader, S.A., Bertand, M. and Wilson, E.H., 2003, Satellite change detection of forest harvest patterns on an industrialized forest landscape. *Forest Science*, **49**.

Schroeder, T.A., Cohen, W.B., Song, C., Canty, M.J. and Yang, Z., 2006, Radiometric correction of multi-temporal Landsat data for characterization of early successional forest patterns in western Oregon. *Remote Sensing of Environment*, **103**, pp. 16–26.

Scott, C.T., Bechtold, W.A., Reams, G.A., Smith, W.D., Westfall, J.A., Hansen, M.H. and Moisen, G.G., 2005, Sample-based estimators used by the Forest Inventory and Analysis National Information Management System. In *The Enhanced Forest Inventory and Analysis Program – National Sampling Design and Estimation Procedures*, P.L. Patterson (Ed.), pp. 43–67 (Asheville, NC: US Department of Agriculture Forest Service, General Technical Report SRS-80).

Scott, R.E. and Mitchell, S.J., 2005, Empirical modelling of windthrow risk in partially harvested stands using tree, neighbourhood, and stand attributes. *Forest Ecology and Management*, **218**, pp. 193–209.

Tomppo, E., Olsson, H., Ståhl, G., Nilsson, M., Hagner, O. and Katila, M., 2008, Combining national forest inventory field plots and remote sensing data for forest databases. *Remote Sensing of Environment*, **112**, pp. 1982–1999.

US Department of Agriculture Forest Service, 1999, Aerial survey standards. Unpublished report (State and Private Forestry, Forest Health Protection). Available online at: http://www.fs.fed.us/foresthealth/technology/pdfs/standards_1099.pdf (accessed 9 December 2008).

US Department of Agriculture Forest Service, 2003, *Forest Inventory and Analysis National Core Field Guide, Volume 1: Field Data Collection Procedures for Phase 2 Plots,*

Version 2.0., pp. 281 (Washington, DC: US Department of Agriculture, Forest Service, Forest Inventory and Analysis).

VALINGER, E. and FRIDMAN, J., 1999, Models to assess the risk of snow and wind damage in pine, spruce, and birch forests in Sweden. *Environmental Management*, **24**, pp. 209–217.

WOODALL, C.W. and NAGEL, L.M., 2007, Downed woody fuel loading dynamics of a large-scale blowdown in northern Minnesota, U.S.A. *Forest Ecology and Management*, **247**, pp. 194–199.